The Characterization of Surface Treated Silica-Filled and Non-Filled Polydimethylsiloxane Films

Michael J. Joyce

Keywords: polydimethylsiloxane (PDMS), surface treatments, uv-ozone, surface energy, wettability, silica-fill, ANOVA, biocompatible

Abstract

In this work, various methods to enable tailoring of polydimethylsiloxane film surfaces are implemented and compared to determine their influence on surface energy and roughness. Films were prepared containing various levels of hydrophilic silica filler. Ultraviolet-ozone, and Piranha solution treatments were also implemented and characterized. Lastly, the combination of both silica filler and treatments were utilized and characterized to understand interactive effects. Influence of filler loading, and surface treatment on roughness, and surface energy of films was determined. Regardless of surface treatment, addition of silica significantly influences total surface energy. Addition of silica influenced total surface energy of the films by itself, and in combination with the Piranha and UV-ozone treatments. The lowest surface energy was that of the control Polydimethylsiloxane film 21.54 N/m. The overall highest surface energy achieved was that of the 10% filled 30-minute Piranha solution treated sample, having a surface energy of 44.14 N/m.

Introduction

PDMS, poly-di-methyl-siloxane, is becoming of increasing interest for use with medical devices and applications (P. Klykken, 2004, Wu et al., 2014). PDMS is highly desirable for such applications due to its high biocompatibility and flexibility enabling its use for both wearable and implantable devices (Ibrahim, 2014, Zheng et al., 2014). Properties that make it desirable for use in these applications also include chemical inertness, thermal stability, gas permeability, and transparency. These properties are a result of its molecular structure as seen in Figure 1.

Western Michigan University

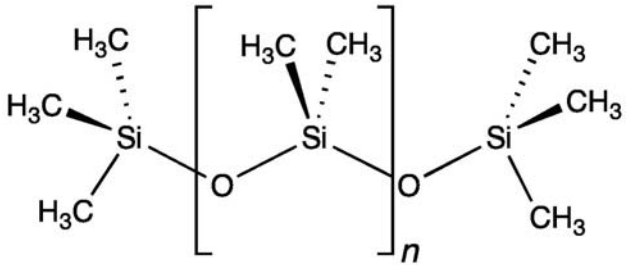

Figure 1. *Molecular structure of PDMS (Smokefoot, 2015)*

However, as a consequence of this molecular structure, the ability of functional inks to wet and adhere to its surface is a challenge. Further, the implementation of its use for such biocompatible printed electronic (PE) systems has been limited due to difficulties involved in the integration, embedding, and/or patterning of (metallic) inks onto its surface due to their weak adhesion to its surface. As contemporary PE is accomplished using additive processes for deposition of materials, one of the main limitations to the use of these substrates (other than the functional characteristics of the created systems) is the ability to properly match ink-substrate properties to optimize interactions enabling desired functional and mechanical properties of the end-use system. The tailoring of substrate properties is essential to the viability of the future of PE. A few of these key substrate surface properties are: porosity, permittivity, smoothness, hydrophobicity/hydrophilicity, surface-free energy, adhesion, water/chemical resistance, and cleanliness. Bulk properties of the substrate materials are also of great importance; these include biocompatibility, glass transition temperature, tensile strength, flexibility, electrical properties, resistance to electric-erosion, and dimensional stability, to name a few. The use of PDMS for the development of functional electronic devices (i.e., sensors) has been of particular interest in recent years; especially, in such applications where implementation of printing techniques may be employed (Mata et al., 2005, B.B. Narakathu, 2014, A. Eshkeiti, 2014). The use of PDMS in such applications is impeded heavily by complications pertaining to its wettability (Shantanu Bhattacharya, 2005, Maji et al., 2012). This is especially true as it pertains to its utilization with high-speed processing techniques. A major challenge resultant of the inability to properly wet PDMS films is the inability to obtain the desired levels of adhesion of materials to the films surface (Oláh et al., 2005, Jovanche Trajkovikj, 2012). This inability to properly adhere materials, most notably metals, to the film surfaces greatly reduces the ability to utilize high-speed processes (i.e., flexographic printing) in the development of functional (electronic) devices. The ability to deposit metallic materials is essential for the creation of the wiring required for such devices. As electrical conductivity is the most important property for wiring materials to have, metallic materials are most often the materials of choice.As the application of biocompatible printed sensors evolves, the need for high efficiency, robust PDMS sensors grows. As a result, there is an increasing need to improve the printability of PDMS, both as the active material in ink and as a substrate for other functional inks. This requires a more comprehensive understanding of the surface treatments

and influence of filler loading on the surface energy and wetting characteristics of PDMS films. PE devices have been developed using screen (Namsoo Lim, 2009), gravure (Erika Hrehorova, 2011, Jinsoo Noh, 2010, Erika Hrehorova, 2007), flexographic (Michael Joyce, 2014, Whitesides, 1998, Patel et al., 2008, Donghak Byun, 2013, M. Brischwein, 2006), and inkjet (Soltman et al., 2010, Sooman Lim, 2013, Moira M. Nir, 2010, Galagan et al., 2013) processes. However, the printing of devices or components has been very limited with regards to the use of PDMS. This is in part due to the known complications pertaining to the wetting and adhesion of metallic particles to PDMS substrates.

One of the essential components for most PE devices is a high functioning electrode; for which a continuous film is needed. Often, Ag is used due to its beneficial properties such as high conductivity and low oxidation, as well as its lower cost in comparison to gold. Copper has also been utilized as it enables high conductivities, however, it does not posses some of the other characteristics desired for use in medical applications. With regards to its use in biomedical applications, it is advantageous to possess high antimicrobial characteristics, which silver delivers. The ability to encapsulate copper particles in silver shells (M. Grouchko, 2009) has recently been shown, and could be beneficial in cases where encapsulation of the device is not needed or desired. Although some researchers have shown the ability to print conductive inks onto PDMS, the need to encapsulate the device was required, to obtain the required robustness and efficiency throughout the lifetime of its use.

Contact angle measurements are widely used for the determination of the wettability of a substrate. It is also a widely used characterization technique for the determination of surface energy and for studying the loss and recovery of the hydrophobicity of silicone rubbers (Wolf, 2010, Mata et al., 2005, Maji et al., 2012, Efimenko et al., 2002). So, this method can be used to accurately measure the wetting characteristic of a PDMS surface. The fundamental equation for measurement of solid surface tension by contact angle measurements is described by the Young equation (Young, 1805). For the evaluation of the surface energy, the contact angles of several kinds of liquids can be measured against the PDMS surfaces, and the critical surface energy estimated using the acquired Zisman-plot (Konrad Kabza, 2000). Although this method is not exactly equal to the solid surface energy, values obtained are useful for comparing the wettability of solid surfaces.

By better characterizing surface treatments and their influence on the wettability of PDMS their effects on the final output can be better understood resulting in a greater ability to properly match the properties between substrate and inks for the creation of more efficient and robust PE devices. While the affects of UVO and Piranha treatments on non-filled PDMS have been reported, a comparison of these treatments to their use with additional levels of modified silica has yet to be

reported. In addition, the effects of these treatments with the additional use of silica filler using various treatment times are new. From these results, those working in the field of PE can advance the wetting and adhesion of conductive metallic films on PDMS. This work aims to advance the knowledge of available surface treatment methods that may be applied to PDMS to raise its surface energy and improve its wettability, and hence printability. The desire to use PDMS as the substrate for biosensors is a driving motivation for this study.

Experimental

PDMS films were prepared using Sylgard-184 (supplied by Dow Corning, Midland, MI), and hydrophobic fumed silica (Degussa, Jetsil® AK 15). PDMS Sylgard-184 is a heat curable PDMS supplied as a two-part kit consisting of pre-polymer (base) and cross-linker (curing agent) components. The manufacturer recommends that the pre-polymer and cross-linker be mixed at a 10:1 weight ratio, respectively. The hydrophobic fumed silica had a particle size of approximately 1.5 microns; as measured by ACCUSIZER 770 (PSS Nicomp). Once mixed, the polymer mix was allowed to degas in ambient conditions for approximately 1 hour, after which time 30 grams was poured into a 17.6 x 11.2mm (L x W) mold. The mold was leveled on a plate and placed onto a leveled shelf within an oven at approximately 140°C for 20 minutes to obtain films of uniform thickness. Once dried, the films were placed in a desiccator and allowed to sit for 24 hours prior to removing them from the mold. The films were then cut into strips (6" X 0.25" L X W) to enable their surface energies to be measured. The surface energy and roughness of filled and non-filled PDMS films were characterized before and after being exposed to two different surface treatments for various periods of time. The two treatments applied were 1) ultraviolet ozone, UVO, ('Jelight' Irvine, CA model 144AX) and 2) submersion in Piranha solution (3:1 ratio of H2O2 and H2SO4). The surface energies of the films were measured using an FTA 200 (First Ten Angstrom Dynamic Contact Angle) measurement apparatus. The Owens-Wendt method was used for determination of the contact angles. It is one of the most common methods used for estimating the surface free energy of solids and the two most frequently used measurement fluids used are water and methylene iodide (diodomethane). This method was used to determine the surface energies of the films. The contact angles of water and methylene iodide were measured with a First Ten Angstrom dynamic contact angle measurement device, which captures the change in contact angle with time with a high-speed video camera (Angstroms, 1998) and (Owens, 1969). The static contact angles (sessile drop method) of two liquids, ultra high filtered deionized water, and methylene iodide were measured. Contact angle measurements were taken on the topside of the PDMS films, that is, the side that was in contact with the air (not the side in contact with the mold). Once captured, the change in contact angle with time was plotted, and the equilibrium contact angle obtained and used in the estimation of the surface energy of the solid to which the liquids were applied. Five contact

angles were obtained for each fluid from which five surface energy values were estimated. The average surface energies (total, polar and dispersive) for each sample are reported.

After completion of these measurements, new strips were taken from the same molded film and were UVO treated using a Jelight® (Irvine, CA) model 144AX UVO cleaner. Samples were subjected to UVO treatment times of 10, 20, 30, and 40, minutes allowing determination of treatment impact on surface energy. Samples also underwent treatment using a Piranha Solution (3:1 concentrated sulfuric acid to 30% hydrogen peroxide solution) soak. These samples were soaked for 10, 20, 30, and 40 minutes to determine treatment impact on surface energy.

The roughnesses of the PDMS films were measured using a Contour GT-K (Bruker Corporation) white-light interferometer. Topographical imaging was carried out in variable scanning interferometry (VSI) mode using a 5X objective giving a sample area of approximately 1.25 mm x 0.98 mm (L X W), and a sampling interval of 2 μm. The surface roughnesses of the samples were obtained in terms of the arithmetic mean of the surface roughness (Sa). Thickness was found using a Mitutoyo (Absolute Digimatic) digital micrometer. Ten measurements from each sample set (% Silica Fill) were taken. Two different sample films per condition were used, having five measurements taken from each.

Results and Discussion

The results of the thickness measurements are shown in Table 1. The results show a decreasing trend in thickness with the addition of silica filler. This is attributed to the silica filler being denser than the PDMS and films having been prepared on a weighted basis would increase in density with the amount of silica added. Due to the care in making the films to ensure the molds and drying trays were level, as shown, the standard deviations of the PDMS films are very low (0.1mm) for all conditions, indicating very good film uniformity for all films.

PDMS Silica Fill (%)	*0*	*5*	*10*
Thickness (mm):	1.5 ± 0.1	1.4 ± 0.1	1.3 ± 0.1

Table 1. *Average Thickness of PDMS Films*

The results of the roughness measurements for the untreated (control sample set) PDMS films are shown in Table 2, topographic images of the surfaces of the untreated 0,5, and 10% silica filled PDMS films are shown in Figures 2-4. The results show the smoothness of the film to decrease significantly upon addition of the 5% silica and only slightly between the 5% and 10% levels of addition (especially when considering the standard deviations). The smaller decrease in roughness between the 5 and 10% addition levels indicates a close packing of the silica particles at the film surface. This packing may also be seen in the topographic images, showing the additional roughness created by the silica. The unfilled sample

also has some roughness to the sample, but this roughness is attributed to surface contamination such as dust, or entrapped air that was released during drying. The higher silica loading may also be more effective in restricting film shrinkage during drying. The low standard deviations in roughness values indicate that the films are uniform, though rough.

PDMS Silica Fill (%)	0	5	10
Roughness (μm)	0.04 ± 0.01	0.10 ± 0.02	0.10 ± 0.01

Table 2. *Average Roughness of PDMS Films (Control)*

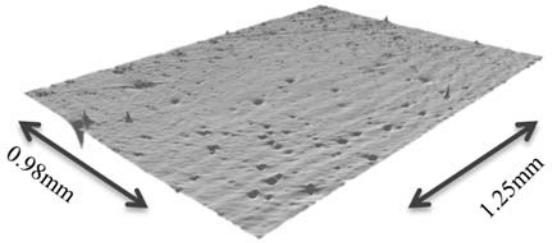

Table 2. *Average Roughness of PDMS Films (Control)*

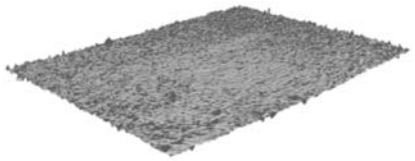

Figure 3. *Topographic Image of 5% Silica Fill PDMS Film (Control)*

Figure 4. *Topographic Image of 10% Silica Fill PDMS Film (Control)*

The results of the roughness measurements obtained by the Piranha solution and UV-ozone treatments are shown in Table 3. The results show the roughness values of the Piranha solution treatments to be very high, for all levels of silica fill and treatment time in comparison to that of the untreated (control) and UV-Ozone treated samples. Piranha solution treatment of the 0% silica filled samples were the highest, and showed a steady increase of roughness with time. The 5 and 10% silica filled samples showed an initial increase in roughness after 10 minutes of Piranha treatment, but did not show any significant increase with increased treatment time until the 40-minute treatment time for the 10% filled sample. This may be attributed to the silica filler retarding the action of the Piranha solution treatment causing a lag in its effects until the 40 minute time period when sufficient amount of the silica had been exposed. Once the silica filler was sufficiently exposed, the Piranha solution was likely able to penetrate passed the silica to the layers of PDMS entrapped below the silica, hence, enabling it to be effected by the solution. Topographic images of the surfaces of the 40 minute Piranha solution treated 0,5, and 10% silica filled PDMS films are shown in Figures 5-7. These results and images show the ferocity of the Piranha solution, and its surface cleaning power. In contrast, the roughnesses of the UV-ozone treated samples were very low. As shown, the values in Table 3 (pertaining to the UV-Ozone samples) remained

unchanged from the control samples in Table 2. From the differences between the two results it is clear that the two treatments modify the surface of the PDMS films differently. That is, the UV-ozone treatment modifies the atomic surface by adding functional (polar) groups to the surface, while the Piranha solution roughens the macro surface. Each treatment works to increase the surface energy of the films in its own way. It is also clear from the images the two ways in which the treatments modify the films surface, although there are no images of the UV-Ozone treated samples as there is no visible difference between these images and the ones presented for the untreated films surfaces.

PDMS Silica Fill	***Piranha** Treatment Time (min)*			
	10	*20*	*30*	*40*
0%	0.94 ± 0.02	1.34 ± 0.05	1.46 ± 0.10	1.70 ± 0.02
5%	0.61 ± 0.01	0.67 ± 0.08	0.65 ± 0.01	0.65 ± 0.03
10%	0.49 ± 0.02	0.46 ± 0.08	0.48 ± 0.04	0.62 ± 0.04
	***UV-Ozone** Treatment Time (min)*			
	10	*20*	*30*	*40*
0%	0.039 ± 0.01	0.039 ± 0.01	0.039 ± 0.01	0.039 ± 0.01
5%	0.10 ± 0.02	0.10 ± 0.02	0.10 ± 0.02	0.10 ± 0.02
10%	0.10 ± 0.01	0.10 ± 0.01	0.10 ± 0.01	0.10 ± 0.01

Table 3. *Average Roughness (μm) of PDMS Films With Treatments*

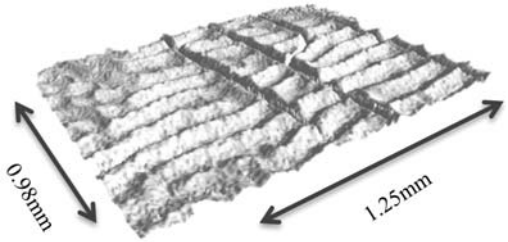

Figure 5. *Topographic Image of 0% Silica Fill PDMS Film (40min Piranha treated)*

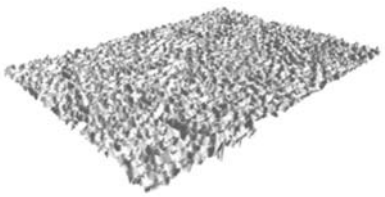

Figure 6. *Topographic Image of 5% Silica Fill PDMS Film (40min Piranha treated)*

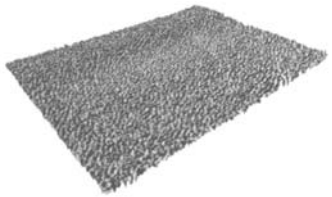

Figure 7. *Topographic Image of 10% Silica Fill PDMS Film (40min Piranha treated)*

To analyze the results of the surface energies, a one-way ANOVA was performed using the Minitab® 17 software package (Minitab Inc.). ANOVAs were performed on the data pertaining to surface energies versus treatment type, treatment time, and level of silica filler added. The results are shown in Table 4. The analysis was performed both with and without the control group's data present. For all ANOVAs,

the null hypothesis was that all means are equal, and the alternative hypothesis was at least one mean is different. A significance level of $\alpha = 0.05$ was used and equal variances were assumed.

	With Control (p-value)	Without Control (p-value)
Total Surface Energy vs. Treatment Type	0.006	0.324
Total Surface Energy vs. Treatment Time (min)	0.009	0.223
Total Surface Energy vs. Silica Fill (%)	0.030	0.006
Polar Component vs. Treatment Type	0.001	0.477
Polar Component vs. Treatment Time (min)	0.000	0.092
Polar Component vs. Silica Fill (%)	0.256	0.063
Dispersive Component vs. Treatment Type	0.156	0.070
Dispersive Component vs. Treatment Time (min)	0.900	0.831
Dispersive Component vs. Silica Fill (%)	0.000	0.000

Table 4. *One-way ANOVA Data*

An examination of the p-values shows all factors to significantly impact the total surface energy of the PDMS films in the presence of the control. However, in the absence of the control data only the percent of silica fill addition is significant. This difference indicates that while treatment type and time significantly alters the total surface energy of the PDMS film, there is an insignificant difference between the total surface energies of the Piranha and UV-ozone samples. Regardless of the surface treatment, the addition of silica significantly influences the total surface energy. A comparison of the p-values for the polar and dispersive forces indicates that the changes in the observed total surface energies are the result of an increase in the polar component and the difference between polar components for both the UV-ozone and Piranha treatments are insignificant. The significance of these findings is further substantiated in Figures 8-10, which show the interactions between the main effect variables. From the total surface energy interaction plot, it is clear that there is a strong interaction between all three main effect variables.

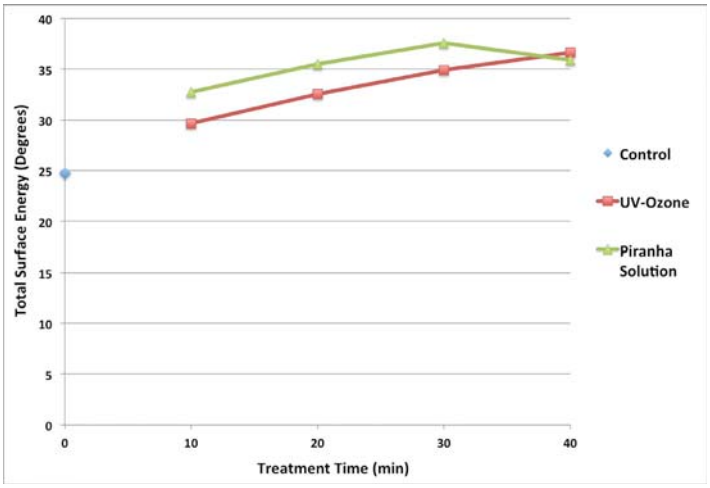

Figure 8. *Interaction Plot Total Surface Energy vs. Treatment Type*

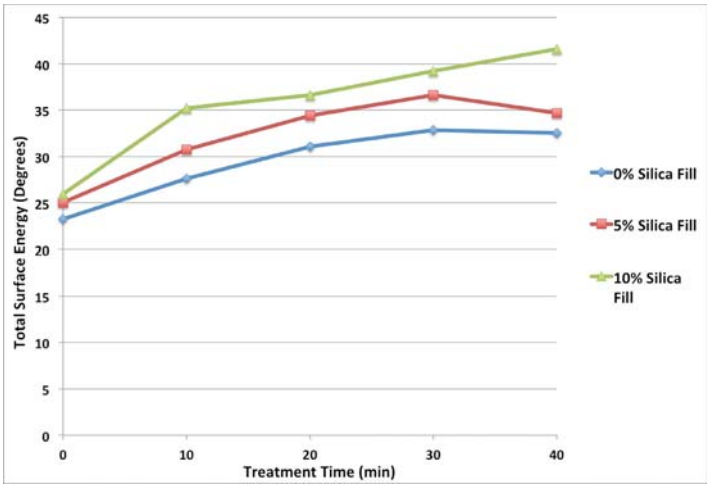

Figure 9. *Interaction Plot Total Surface Energy vs. Time (min)*

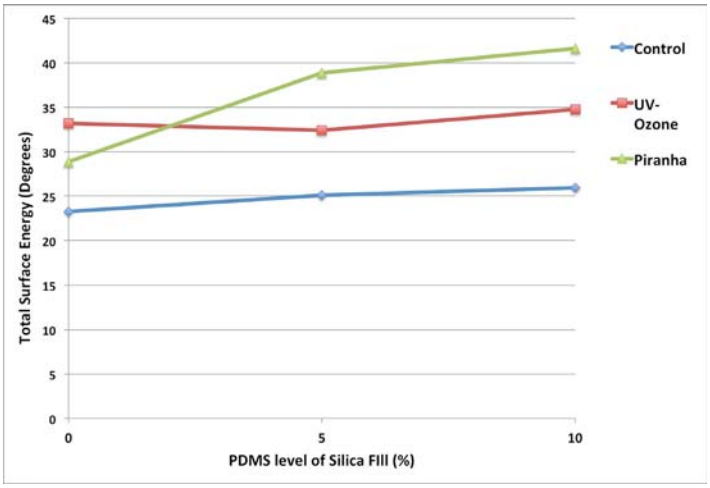

Figure 10. *Interaction Plot Total Surface Energy vs. % Silica Fill*

After treatment, the surface energies of the films were again estimated. An aging study showed no immediate change within surface energies of the samples over a 20-minute period of time. After performing the surface energy estimation, the roughnesses of the films were then measured. Further ageing studies were performed after 24 hours (post treatment). These results showed the complete reversal of surface energy for the UVO treated samples, while there was no measureable impact of surface energy for the Piranha solution treated samples. A regression analysis was also performed for the surface energy versus treatment time, % silica fill, and treatment type. These results can be found in the Appendix.

Conclusions

The lowest total surface energy was that of the control PDMS film 21.54 mN/m. The overall highest surface energy achieved was that of the 10% filled 30-minute Piranha solution treated sample, having a total SE of 44.14 mN/m. The Piranha solution changes the macroscopic physical surface in a much more significant way as compared to the UV-ozone treatment. The difference in how the two treatments modify the films surfaces may be seen in the topographic images presented. Both treatments influenced the total surface energy of the PDMS films by changing the polar component. The addition of silica influenced the total surface energy of the PDMS films by itself, and in combination with the Piranha and UV-ozone treatments. An aging study showed no immediate change within surface energies of the samples over a 20-minute period of time. The addition of the silica filler did not provide any positive impact of the influence of the treatments to the surface energies with time. PDMS films of similar surface energy can be obtained both with and without roughening of the surface. This may be achieved by varying the treatment type and time in the presence of silica filler. The immense amount of roughening caused by the Piranha solution would likely cause the films to be unusable for use with most printing processes. It was also seen that the Piranha solution treated samples became dried at their surface, likely affecting their mechanical (i.e., tensile strength) properties. These findings can be valuable to printers seeking to fabricate electronic sensors on PDMS films. Through the combination of roughness and surface energy variations the wetting and adhesion properties of functional inks can be manipulated to enhance sensor performance and durability. PDMS is a substrate of high interest for such applications due to its biocompatibility and this work demonstrates that with proper surface treatment or modification there is potential for its use.

References

A. ESHKEITI, B. B. N., A.S.G. REDDY, S. EMAMIAN, M.K. JOYCE, B.J. BAZUIN, M.Z. ATASHBAR 2014. Screen Printed Flexible Capacitive Pressure sensor. 13th IEEE Sensors Conference. Valencia, Spain.

ANGSTROMS, F. T. 1998. Owens-Wendt Surface Energy Calculation [Online]. Available: http://www.firsttenangstroms.com/pdfdocs/OwensWendtSurface EnergyCalculation [Accessed August 16, 2015 2015].

B.B. NARAKATHU, A. S. G. R., A. ESHKEITI, S. EMAMIAN, M.Z. ATASHBAR 2014. Development of a Novel Printed Flexible Microfluidic Sensing Platform Based on PCB Technology. 13th IEEE Sensors Conference. Valencia, Spain.

DONGHAK BYUN, S. J. C., AND SOHEE KIM 2013. Fabrication of a flexible penetrating microelectrode array for use on curved surfaces of neural tissues. Journal of Micromechanics and Microengineering, 23, 1–10.

EFIMENKO, K., WALLACE, W. E. & GENZER, J. 2002. Surface Modification of Sylgard-184 Poly(dimethyl siloxane) Networks by Ultraviolet and Ultraviolet/ Ozone Treatment. Journal of Colloid and Interface Science, 254, 306-315.

ERIKA HREHOROVA, A. P., V.N. BLIZNYUK, AND PAUL D. FLEMING 2007. Polymeric Materials for Printed Electronics and Their Interactions with Paper Substrates. 23rd International Conference on Digital Printing Tech NIP.

ERIKA HREHOROVA, M. R., ALEXANDRA PEKAROVICOVA, BRADLEY BAZUIN, AMRITH RANGANATHAN, SEAN GARNER, MEMBER, IEEE, GARY MERZ, JOHN TOSCH, AND ROBERT BOUDREAU 2011. Gravure Printing of Conductive Inks on Glass Substrates for Applications in Printed Electronics. JOURNAL OF DISPLAY TECHNOLOGY, 7, 318-324.

GALAGAN, Y., COENEN, E. W. C., ABBEL, R., VAN LAMMEREN, T. J., SABIK, S., BARINK, M., MEINDERS, E. R., ANDRIESSEN, R. & BLOM, P. W. M. 2013. Photonic sintering of inkjet printed current collecting grids for organic solar cell applications. Organic Electronics, 14, 38-46.

IBRAHIM, K. M. N. K. K. 2014. Development of a low cost roll-to-roll nanoimprint lithography system for patterning 8-inch wide flexible substrates. International Journal of Nanotechnology 11, 520 - 528.

JINSOO NOH, D. Y., CHAEMIN LIM, HWAJIN CHA, JUKYUNG HAN, JUNSEOK KIM, YONGSU PARK, VIVEK SUBRAMANIAN, AND GYOUJIN CHO 2010. Scalability of Roll-to-Roll Gravure-Printed Electrodes on Plastic Foils. IEEE TRANSACTIONS ON ELECTRONICS PACKAGING MANUFACTURING, 33.

JOVANCHE TRAJKOVIKJ, J.-F. Z. R., AND ANJA K SKRIVERVIK 2012. Soft and Flexible Antennas on Permittivity Adjustable PDMS Substrates. Loughborough Antennas & Propagation Conference. Loughborough, UK: IEEE.

KONRAD KABZA, J. E. G., AND JESSICA L. MCGRATH 2000. Contact Angle Goniometry as a Tool for Surface Tension Measurements of Solids, Using Zisman Plot Journal of Chemical Education, 77, 63-65.

M. BRISCHWEIN, S. H., W. VONAU, F. BERTHOLD, H. GROTHE, E.R. MONTRESCU, AND B. WOLF 2006. Electric cell-substrate impedance sensing with screen printed electrode structures. Lab on a Chip, 6, 819-822.

M. GROUCHKO, A. K. A. S. M. 2009. Formation of air-stable copper–silver core–shell nanoparticles for inkjet printing. Journal of Materials Chemistry 19, 3057-3062.

MAJI, D., LAHIRI, S. K. & DAS, S. 2012. Study of hydrophilicity and stability of chemically modified PDMS surface using piranha and KOH solution. Surface and Interface Analysis, 44, 62-69.

MATA, A., FLEISCHMAN, A. & ROY, S. 2005. Characterization of Polydimethylsiloxane (PDMS) Properties for Biomedical Micro/Nanosystems. Biomedical Microdevices, 7, 281-293.

MICHAEL JOYCE, S. G. R. A., SEPEHR EMAMIAN, DR. MASSOOD ATASHBAR, DR. PAUL D. FLEMING III, AND TONY DONATO 2014. Contribution of Flexo Process Variables to Fine Line Ag Electrode Performance. International Journal of Engineering Research & Technology 3, 1645-1656.

MOIRA M. NIR, D. Z., ILANA HAYMOV, LIMOR BEN-ASHER, ORIT COHEN, BILL FAULKNER, AND FERNANDO DE LA VEGA 2010. Electrically conductive inks for inkjet printing In: MAGDASSI, S. (ed.) The chemistry of inkjet inks. World Scientific: New Jersey-London Singapore.

NAMSOO LIM, J. K., SOOJIN LEE, NAMYOUNG KIM, GYOUJIN CHO 2009. Screen printed resonant tags for electronic article surveillance tags. IEEE Trans. Adv. Packaging, 32, 72-76.

OLÁH, A., HILLBORG, H. & VANCSO, G. J. 2005. Hydrophobic recovery of UV/ozone treated poly(dimethylsiloxane): adhesion studies by contact mechanics and mechanism of surface modification. Applied Surface Science, 239, 410-423.

OWENS, D. K. A. W., R. C. 1969. Estimation of Surface Free Energy of Polymers. Journal of Applied Polymer Science, 13, 1741-1747.

P. KLYKKEN, M. S., X. THOMAS 2004. Silicone Film-Forming Technologies for Health Care Applications. Dow Corning: Dow Corning.

PATEL, J. N., KAMINSKA, B., GRAY, B. L. & GATES, B. D. 2008. PDMS as a sacrificial substrate for SU-8-based biomedical and microfluidic applications. Journal of Micromechanics and Microengineering, 18.

SHANTANU BHATTACHARYA, A. D., JORDAN M. BERG, AND SHUBHRA GANGOPADHYAY 2005. Studies on Surface Wettability of Poly(Dimethyl) Siloxane (PDMS) and Glass Under Oxygen-Plasma Treatment and Correlation With Bond Strength. MicroElectro Mechanical Systems, 14, 590-597.

SMOKEFOOT. 2015. PDMS Molecular Structure [Online]. Available: href="https://commons.wikimedia.org/wiki/File:PmdsStructure.png - /media/File:PmdsStructure.png"

SOLTMAN, D., SMITH, B., KANG, H., MORRIS, S. J. & SUBRAMANIAN, V. 2010. Methodology for inkjet printing of partially wetting films. Langmuir, 26, 15686-93.

SOOMAN LIM, M. J., PAUL D. FLEMING, AHMED TAUSIF AIJAZI, AND MASSOOD ATASHBAR 2013. Inkjet Printing and Sintering of Nano-Copper Ink. Journal of Imaging Science and Technology.

WHITESIDES, Y. X. A. G. M. 1998. Angewandte Chemie International Edition 37, p. 550–575

WOLF, R. 2010. Role of Plasma Surface Treatments on Wetting and Adhesion. Engineering, 02, 397-402.

WU, J., WANG, R., YU, H., LI, G., XU, K., TIEN, N. C., ROBERTS, R. C. & LI, D. 2014. Inkjet-printed microelectrodes on PDMS as biosensors for functionalized microfluidic systems. Lab Chip.

YOUNG, T. 1805. An Essay on the Cohesion of Fluids. Philosophical Transactions Royal Society of London, 95, 65-87.

ZHENG, Q., SHI, B., FAN, F., WANG, X., YAN, L., YUAN, W., WANG, S., LIU, H., LI, Z. & WANG, Z. L. 2014. In vivo powering of pacemaker by breathing-driven implanted triboelectric nanogenerator. Adv Mater, 26, 5851-6.

Appendix

Regression Analysis: Surface Energy versus Treatment Time, % Silica Fill, Treatment Type:

Method: Categorical predictor coding (1, 0)

Source	DF	Adj SS	Adj MS	F-Value	P-Value
Regression	4	566.94	141.74	13.78	0.000
Treatment Time	1	91035	91035	8.88	0.007
% Silica Fill	1	200.67	200.67	19.52	0.000
Treatment Type	2	72.71	36.36	3.54	0.470
Error	22	226.20	10.28		
Total	26	793.15			

*Computed using alpha = 0.05

Model Summary

S	R-sq	R-sq(adj)	R-sq(pred)
3.20656	71.48%	66.29%	57.43%

Coefficients

Term	Coef	SE Coef	T-Value	P-Value	VIF
Constant	21.39	2.00	10.70	0.000	
Treatment Time	0.1745	0.0585	2.98	0.007	1.56
% Silica Fill	0.668	0.151	4.42	0.000	1.00
Treatment Type					
Piranha	6.34	2.54	2.50	0.200	4.17
UV-Ozone	4.35	2.54	1.71	0.101	4.17

Treatment Type	Regression Equation
None	Surface Energy= 21.39 + 0.1745(Treatment Time) + 0.668(% Silica Fill)
Piranha	Surface Energy = 27.73 + 0.1745(Treatment Time) + 0.668(% Silica Fill)
UV-Ozone	Surface Energy = 25.74 + 0.1745(Treatment Time) + 0.668(% Silica Fill)

Water Contact Angle		Methylene Iodide Contact Angle		Treatment Type	Treatment Time (min)	Silica Fill (%)
STD (±)	*Average*	STD (±)	*Average*			
2.3	98.5	1.8	66.5	Control		0
1.4	92.4	1.2	65.8	Control		5
3.7	96.2	1.3	64.6	Control		10
3.1	84.8	1.2	63.6	Uv-Ozone	10	0
0.0	80.1	0.1	63.3	Uv-Ozone	10	5
2.7	80.7	0.6	62.3	Uv-Ozone	10	10
1.0	70.2	1.7	66.6	Uv-Ozone	20	0
0.1	79.5	0.1	61.4	Uv-Ozone	20	5
1.0	76.7	0.6	61.5	Uv-Ozone	20	10
0.7	70.3	3.2	63.9	Uv-Ozone	30	0
0.1	73.6	0.1	55.8	Uv-Ozone	30	5
1.3	72.5	2.2	53.2	Uv-Ozone	30	10
0.9	69.3	2.5	65.1	Uv-Ozone	40	0
0.2	81.7	0.1	55.9	Uv-Ozone	40	5
1.8	62.4	1.8	53.4	Uv-Ozone	40	10
2.5	85.1	3.1	67.7	Piranha Solution	10	0
1.2	81.3	2.3	59.3	Piranha Solution	10	5
7.5	69.2	2.5	48.0	Piranha Solution	10	10
2.9	80.3	5.4	70.3	Piranha Solution	20	0
3.3	72.3	2.9	51.3	Piranha Solution	20	5
3.8	65.6	1.7	51.5	Piranha Solution	20	10
2.9	77.6	3.7	64.4	Piranha Solution	30	0
2.9	74.1	2.4	50.1	Piranha Solution	30	5
3.7	67.3	2.7	38.8	Piranha Solution	30	10
3.2	78.9	4.3	66.9	Piranha Solution	40	0
3.0	73.9	1.6	52.2	Piranha Solution	40	5
6.2	65.9	8.7	50	Piranha Solution	40	10

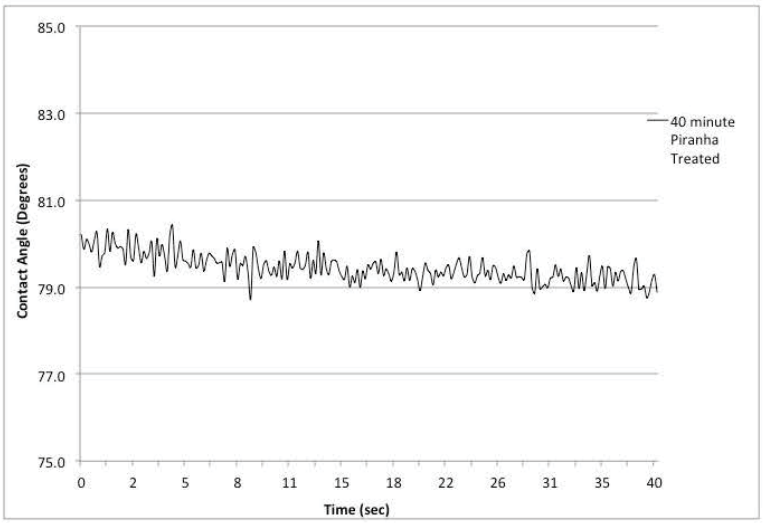

Total Surface Energy			Polar Component			Dispersive Component			Treatment Type	Treatment Time (min)	Silica Fill (%)
(-) Average	Average	(+) Average	(-) Average	Average	(+) Average	(-) Average	Average	(+) Average			
22.0	21.54	21.2	0.7	0.56	0.4	21.3	20.98	20.8	Control		0
25.9	25.03	25.6	3.3	2.85	3.1	22.6	22.18	22.6	Control		5
27.0	25.98	25.2	2.7	1.77	1.0	24.2	24.22	24.2	Control		10
29.9	28.46	27.1	7.4	6.08	4.8	22.5	22.38	22.3	Uv-Ozone	10	0
30.2	30.2	30.2	8.6	8.62	8.6	21.7	21.58	21.6	Uv-Ozone	10	5
31.6	30.34	29.2	9.5	8.02	6.7	22.1	22.33	22.5	Uv-Ozone	10	10
35.3	34.29	33.3	16.8	16.58	16.4	18.5	17.71	16.9	Uv-Ozone	20	0
31.2	31.13	31.1	8.5	8.50	8.5	22.7	22.63	22.6	Uv-Ozone	20	5
32.9	32.25	31.8	10.7	10.27	9.6	22.1	21.99	22.2	Uv-Ozone	20	10
34.7	34.84	33.7	17.1	15.55	16.2	17.5	19.29	17.6	Uv-Ozone	30	0
35.6	35.57	35.4	10.8	10.75	10.7	24.8	24.82	24.9	Uv-Ozone	30	5
38.3	34.27	35.6	11.1	13.13	10.5	27.2	21.14	25.1	Uv-Ozone	30	10
36.3	35.17	34.1	16.6	16.76	17.0	19.7	18.41	17.1	Uv-Ozone	40	0
43.6	32.64	32.6	6.2	6.07	6.0	26.5	26.57	26.6	Uv-Ozone	40	5
28.8	47.09	40.6	19.0	18.14	17.3	24.6	23.94	23.2	Uv-Ozone	40	10
32.6	26.74	24.7	7.5	6.84	6.2	21.3	19.90	18.5	Piranha Solution	10	0
44.6	31.32	30.0	7.3	6.99	6.9	25.5	24.33	23.1	Piranha Solution	10	5
30.8	40.20	36.4	16.2	11.65	7.6	28.4	28.55	28.8	Piranha Solution	10	10
40.2	27.83	25.0	10.8	10.42	10.1	20.0	17.41	14.8	Piranha Solution	20	0
43.4	37.72	35.3	11.9	10.45	9.1	28.2	27.28	26.2	Piranha Solution	20	5
33.4	40.96	38.7	16.9	14.61	12.6	26.6	26.35	26.1	Piranha Solution	20	10
39.5	30.89	28.4	11.4	10.49	9.7	22.1	20.40	18.8	Piranha Solution	30	0
46.5	37.01	35.4	10.3	9.32	7.9	29.2	27.68	27.6	Piranha Solution	30	5
32.4	44.14	41.8	33.8	10.83	9.1	12.7	33.32	32.7	Piranha Solution	30	10
32.4	29.50	26.8	11.2	10.35	9.5	21.1	19.16	17.3	Piranha Solution	40	0
38.6	36.75	35.0	11.2	9.66	8.2	27.4	27.09	26.8	Piranha Solution	40	5
46.8	41.11	35.3	16.6	14.46	12.6	30.2	26.65	22.7	Piranha Solution	40	10